

Dynamics of highly charged ions in ultraintense laser fields

Zhaoyan Zhou, Zengxiu Zhao and Jianmin Yuan

Department of Physics, National University of Defense Technology, Changsha 410073, People's Republic of China

E-mail: jmyuan@nudt.edu.cn

Received 18 March 2011

Accepted for publication 18 March 2011

Published 20 June 2011

Online at stacks.iop.org/PhysScr/T144/014048

Abstract

The dynamics of highly charged ions in a strong laser field are investigated by solving the two-dimensional time-dependent Dirac equation. Relativistic effects are discussed for the hydrogen-like ions with nuclear charges of $Z = 4, 24$ and 79 by considering the changes in the electron trajectory and coherent emission spectrum with changes in the frequency and intensity of the laser field. With increasing Z , the relative field strength between the ionic core and laser fields changes and this results in different characteristics of the dynamical electronic trajectory as well as the corresponding emission spectrum. For an infrared laser field of strength $E = 8.0$ au, the tunneling ionization can hardly be seen for the hydrogen-like ions of $Z = 24$ and only the resonant multiphoton emission spectra below the ionization threshold are predicted. The above threshold harmonics need more intense laser fields or a higher photon energy.

PACS numbers: 32.80.Rm, 42.50.Hz, 42.65.Ky

(Some figures in this article are in colour only in the electronic version.)

1. Introduction

Over the last 20 years, the perturbation theory is no longer valid for describing the interaction between a strong laser field and atoms. However, most of the strong-field nonlinear phenomena in experiments, including high-order harmonic generation (HHG) [1–3], above-threshold ionization (ATI) [4, 5], hyper-Raman lines [6, 7] and tunneling ionization [8], can still be explained by solving the time-dependent Schrödinger equation (TDSE). Nowadays, the strength of laser field up to 10^{22} W cm⁻², which is much higher than that of a one atomic unit (au) field (3.51×10^{16} W cm⁻²) experienced by an electron in the first Bohr orbital of the hydrogen atom, is available [9, 10]. In such an ultraintense laser field, the dynamical interaction process cannot be described any more using the TDSE because of the non-negligible relativistic effect. It is believed that the relativistic effect has an important role when the following condition is satisfied [11]:

$$U_p = \frac{e^2 E^2}{4m\omega^2} \sim mc^2 \quad \text{or} \quad v = \frac{eE}{m\omega} \sim c, \quad (1)$$

where c is the speed of light.

The dynamics of electrons in a strong laser field are often comprehended by the three-step model [12] without considering the relativistic effect: one electron is first ionized by the laser field and then accelerated in the field; when the direction of the electric field is reversed, the electron can be driven back to its parent ion, where it recombines with the initial state and emits its energy as a harmonic photon. It is predicted in this model that the cutoff energy of the HHG is $I_p + 3.17U_p$, where I_p is the ionization potential of the atom and U_p is the pondermotive energy of an electron in the laser field. It can be seen from the three-step model that the plateau part in the emission spectrum can be extended by using a system with a large ionization potential or by increasing the intensity of the laser field. However, the electron will be ionized too quickly to recombine to the parent ion by using only the ultraintense laser field. The application of a highly charged ion is an effective means for the electron to obtain enough high energy before being ionized in the strong laser field [13–15]. For example, the electron of hydrogen-like uranium in the first Bohr orbit may experience an electric intensity of the order of 10^{29} W cm⁻² before being ionized. The laser field achieved today can only induce the electrons departing from the ionic nucleus temporarily and a high

percentage of the electrons can come back to the ion and emit the energy obtained from the laser field.

In the present study, the electronic dynamics of highly charged ions in an ultraintense laser field is investigated by solving the time-dependent Dirac equation (TDDE) to include the relativistic effect automatically. This full relativistic method, which was developed in 1999 by Braun *et al* [16], has a unique superiority in treating many relativistic problems [17, 18]. Here we use this method to simulate the dynamics of highly charged ions and make some comparisons with the results obtained from the non-dipole TDSE in order to show the changes induced by the high-order relativistic effect.

2. Numerical methods

In the ultraintense laser field, the electron can be accelerated up to a speed comparable to the speed of light and the magnetic effect is no longer negligible. To describe the forces induced by the magnetic field, we must perform calculations at least in two dimensions. Taking the ground state of the ion as the initial state, the magnetic quantum number should be set to zero in the linearly polarized laser field used throughout this work. So, we can obtain accurate results by solving the two-dimensional (2D) Dirac equation:

$$i\frac{\partial}{\partial t}\Psi(x, z, t) = \left\{ c\alpha \cdot \left[\mathbf{p} - \frac{1}{c}\mathbf{A}(z, t) \right] + c^2\beta + V(x, z) \right\} \Psi(x, z, t). \quad (2)$$

The movement of the electron is restricted in the (x, z) plane here. $\Psi(x, z, t) = (\varphi_1, \varphi_2, \varphi_3, \varphi_4)^*$ is the four-component Dirac spinor; α and β are the 4×4 Dirac matrices. $V(x, z)$ describes the ionic potential. The soft Coulomb potential [19, 20] is adopted to eliminate the singularity of the Coulomb potential for the numerical calculation. The potential describing the hydrogen-like ion with nuclear charge Z is of the form

$$V(x, z) = -\frac{Z}{\sqrt{x^2 + z^2 + a}}, \quad (3)$$

with $a = 0.64/Z^2$.

In equation (2), $\mathbf{A}(z, t)$ is used to describe the vector potential of the incident laser field. Here we consider only the laser field linearly polarized along the x -axis and propagating along the z -axis, i.e.

$$E_x(x, t) = Ef(z, t) \cos(\omega t - \omega z/c), \quad (4)$$

where E and ω are the amplitude and frequency of the incident laser field, respectively. $f(z, t)$ is the profile of the laser pulse, which is chosen to be one with a 3 optical cycle (o.c.) linearly turn-on followed by a constant part for the rest of the pulse,

$$E_x(z, t) = \begin{cases} E \frac{t - z/c}{3T} \cos(\omega t - \omega z/c), & 0 < t - z/c \leq 3T, \\ E \cos(\omega t - \omega z/c), & 3T < t - z/c < T_{\max}, \end{cases} \quad (5)$$

where $T = 2\pi/\omega$ denotes 1 o.c. Here, T_{\max} is the total interaction time calculated here. The corresponding vector potential can be expressed as

$$A_x(z, t) = -c \int_0^t E_x(z, t') dt' = \begin{cases} -\frac{cE}{\omega(3T)} \left\{ \frac{(t - z/c) \sin(\omega t - \omega z/c)}{\omega} + \frac{1}{\omega} [\cos(\omega t - \omega z/c) - 1] \right\}, & 0 < t - z/c \leq 3T, \\ -\frac{cE}{\omega(3T)} \sin(\omega t - \omega z/c), & 3T < t - z/c < T_{\max}. \end{cases} \quad (6)$$

The magnetic field B is parallel to the y -axis, i.e. perpendicular to the xz plane where we perform the calculations, and has the same expression as equation (5) for the electric field.

To identify the relativistic effect, we also calculate the corresponding non-relativistic cases by solving the TDSE for the comparison. For the laser field that is not very strong, the dipole approximation TDSE of the following form is usually used for the analysis of the electron dynamical process:

$$i\frac{\partial}{\partial t}\psi(x, z, t) = \left[\frac{\mathbf{p}^2}{2} - \frac{1}{c}\mathbf{p} \cdot \mathbf{A}(t) + V(x, z) \right] \psi(x, z, t). \quad (7)$$

In the dipole approximation, the magnetic part of the laser pulse is omitted and the electron performs a quiver motion exclusively in the direction of the laser polarization. The non-dipole TDSE is as follows:

$$i\frac{\partial}{\partial t}\psi(x, z, t) = \left[\frac{(\mathbf{p} - A_x(z, t)/c)^2}{2} + V(x, z) \right] \psi(x, z, t). \quad (8)$$

It can also include the first order relativistic correction. We will make some comparisons in the results obtained with equations (2), (7) and (8) to analyze the relativistic effects more clearly. Atomic units (au) are used throughout this paper unless specially mentioned.

3. Competition between the nuclear and the laser field

The dynamics of the electron in the ultraintense laser field can be reflected intuitively in its spatial distribution in both the polarization and propagation directions of the laser field. The expectation value of the electron spatial distribution can be obtained via

$$\langle r_i(t) \rangle = \langle \Psi(x, z, t) | r_i | \Psi(x, z, t) \rangle, \quad r_i = x \text{ or } z. \quad (9)$$

It was found by solving the non-dipole TDSE that the magnetic-field-induced drift effect [21, 22] can push the electron away in the propagation direction for the hydrogen atom with $Z = 1$. Our full relativistic results are very similar to those previous results. So it could be expected that the high-order relativistic effect is not important for this case. The magnetic field is reflected more obviously in the drift effect than in the Lorentz force that makes the electron oscillate along the z -axis.

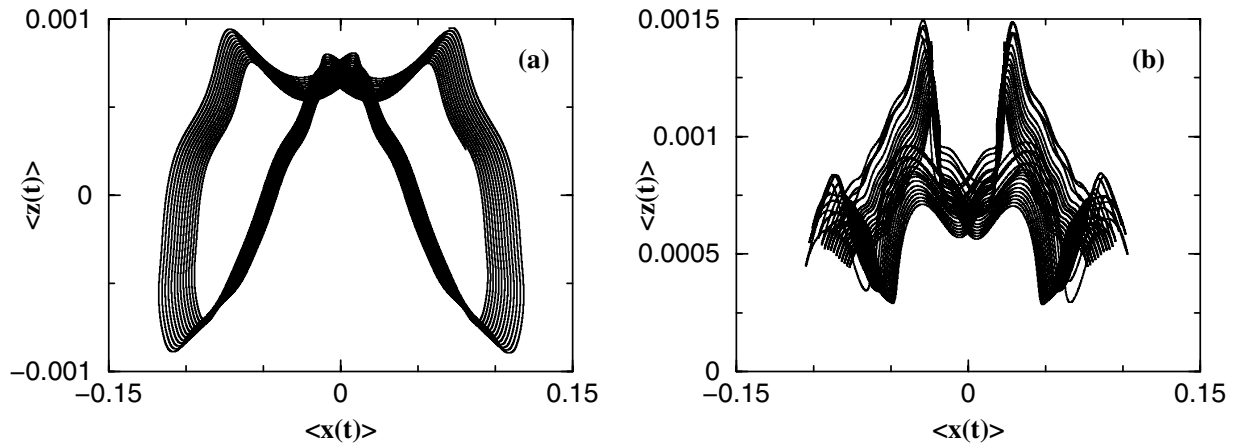


Figure 1. The electronic trajectory calculated from the non-dipole TDSE (a) and TDDE (b) for the ion with potential $V(x, z) = -4/\sqrt{x^2 + z^2 + 0.04}$. The frequency and the electric strength are set to be $\omega = 1.0$ au and $E = 3.0$ au, respectively.

To avoid the strong ionization induced by the drift effect, one can employ the highly charged ion that has the superiority of restraining the electron in the ionic potential. With $Z = 4$, the attractive potential of the nucleus is much stronger than that in neutral atomic hydrogen. The electron can move like the ‘figure of 8’ because of the Lorentz force in the propagation direction as shown in figure 1(a) by solving the non-dipole TDSE, while the same electronic trajectory is predicted quite differently using the TDDE as shown in figure 1(b).

It was shown [13, 23] that the magnetic field component will turn out to be large when the electron approaches the ionic core; then an extreme strong Lorentz push on the wave packet around the ionic core in the laser propagation direction arises and results in a hole around the ionic nucleus. From the viewpoint of electronic spacial distribution, the existence of a hole around the nucleus means that there must be a phase lag between the wave packet motion and the laser field. In other words, the electron cannot arrive at the origin at the same time in the two directions. When the electron is dragged out by the laser field, the strong ionic core field here may retard this movement. Of course, the attractive force from the ionic core can also speed up the process when the electron is driven towards the ionic core. As a result, competition between the nuclear Coulomb field and the laser field can affect the time when the electron passes through the ionic core. The drift effect can also affect the time when the electron comes back to the origin in the propagation direction. It should also be stressed that the competition cannot hold unchanged during the turn-on of the laser field, and the phase lag may be developed during this process. Based on the statements above, the ionization energy, the ionic radius and the frequency and intensity of the laser field all can affect the phase lag that induces the hole around the origin of the ion.

Changes in the dynamical characteristics with the changes in the laser intensity are shown in figure 2 for $Z = 24$. The ionization probability remains zero for a relatively weak laser field. Because of the small ionic radius and large velocity of the electron, we cannot see the phase lag as well as the probability distribution hole. So the trajectory of the electron is just like the ‘figure of 8’ as is shown in figure 2(a). Figure 2(b) is the electronic trajectory with a more intense

laser field. The competition between the ionic core and the laser field can be seen more clearly here, in particular shown by the oscillations in the polarization direction. The electron can pass through the ion core region with high speed under such an intense laser field along the polarization direction. Then the direction of the electric field changes and the electron is slowed down. The strong attraction of the ionic core then plays an important role in stopping the electron from moving so far away from the nucleus. The electron can be decelerated to zero velocity and changes its direction before the maximum of the electric field is reached. So the electron has a high probability of staying around the ionic core in the polarization direction. This competitive process is also reflected in the propagation direction as some small wiggles far from the nucleus.

Taking $\omega = 1.0$ au again, the time-dependent displacement along the x and z axis is shown in figure 3(a) for $Z = 79$. One can see that the strong attractive force from the nucleus plays such an important role that the small wiggles caused by the competition between the ionic nuclear field and the laser field exist all the time during the interaction process. One can hardly see the periodic oscillations, especially in the propagation direction, and the displacement in this direction can be comparable to that in the polarization direction. It was stated in [24] that the small wiggles at times when the electron goes through zero are related to the emission of the non-tunneling harmonics. It is also true here. The strong attractive force from the nucleus here makes it hard to find a proper laser strength to observe the emission spectrum above the threshold when $\omega = 1.0$ au. The above-threshold harmonic generation can only be seen with much higher intensities or high enough frequencies of the laser field. The regular movement of the electron can be seen for $\omega = 10.0$ au and $E = 3500$ au shown in figure 3(b). The laser field is now strong enough to force the electron sufficiently far away from the ionic nucleus and then the electron oscillates with the frequency of the laser field. Then we can see the above-threshold harmonics.

4. Coherent emission spectrum

It was mentioned above that the electron can wiggle around the ionic core only when the photon energy of the laser

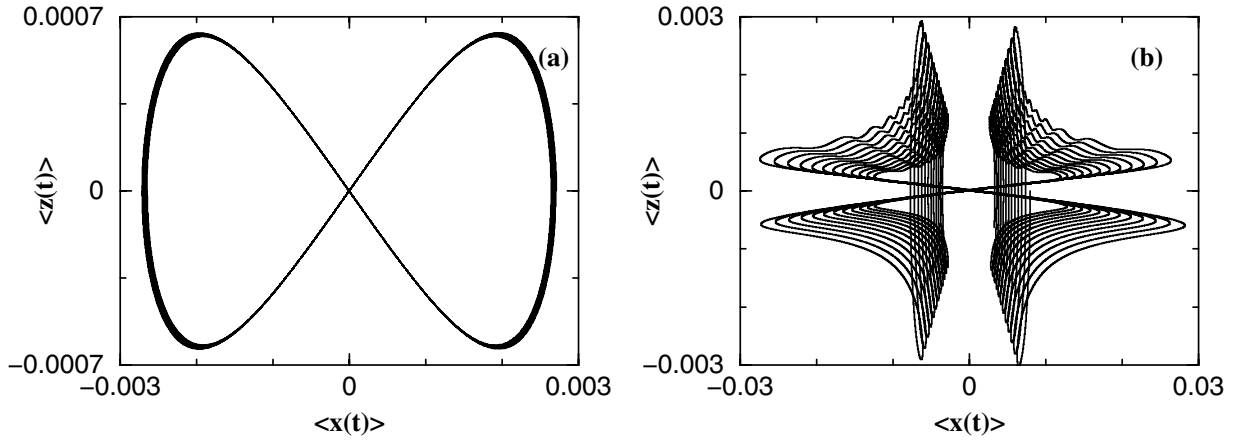


Figure 2. The electronic trajectory calculated from the TDDE for the ion with potential $V(x, z) = -24/\sqrt{x^2 + z^2 + 0.001}$. The frequency and the electric strength are set to $\omega = 1.0$ au and (a) $E = 100$ au and (b) $E = 300$ au.

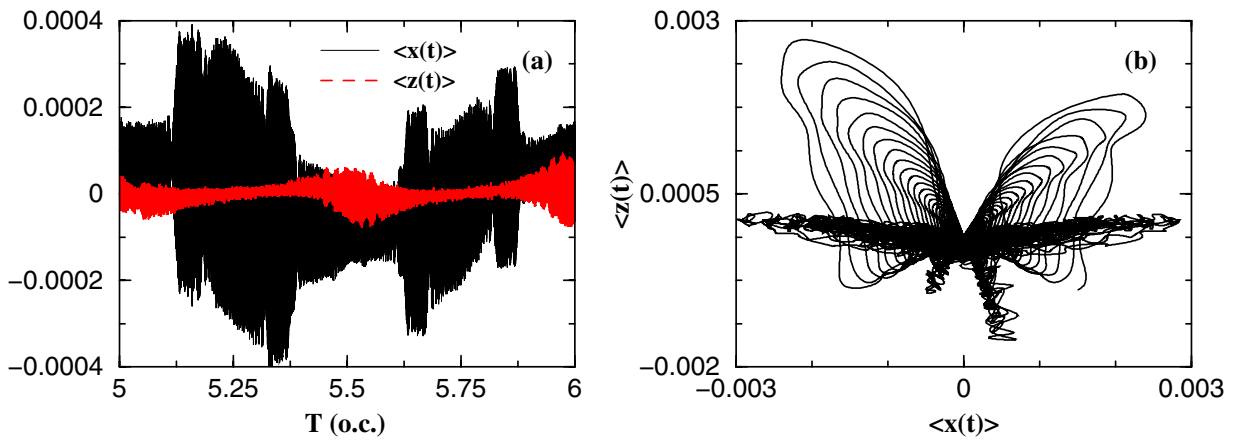


Figure 3. (a) The time-dependent displacement in the polarization (black solid line) and the propagation direction (red dashed line) for the ionic model $V(x, z) = -79/\sqrt{x^2 + z^2 + 10^{-4}}$. The frequency and the electric strength are set to $\omega = 1.0$ au and $E = 500$ au, respectively. (b) The electronic trajectory in the laser field of $\omega = 10.0$ au and $E = 3500$ au.

field is small compared to the ionization energy. Because of the strict requirement on the time step, we have only solved the 1D TDDE for the coherent emission spectrum of a $Z = 24$ hydrogen-like ion in an infrared laser field. Although the magnetic field effect in the propagation direction cannot be included in the 1D calculations, we can qualitatively investigate the basic features of the emission spectrum for highly charged ions with the 1D model:

$$V(x) = -\frac{Z}{\sqrt{x^2 + 2/Z^2}}. \quad (10)$$

The emission spectrum of the hydrogen-like ion with $Z = 24$ in the 800 nm infrared laser field is presented in figure 4(a). The electric strengths are set to be $E = 6.0$ and 8.0 au separately. The energy of the emitted photon is as high as 254 au, about 4456 times the photon energy of the incident laser field. We can only see the resonant multi-photon emissions here. There are also odd order harmonics of about fifth order appearing and decreasing exponentially with increasing harmonic order. Therefore, it is hard for the electron to absorb more photons and emit high-order harmonics unless a resonant transition between the real dressed energy states happens. It can be seen from figure 4(a)

that the transitions are mainly between the ground state and excited states. The transition probabilities between the states 0-1, 1-2 and 0-3 are reduced when the electric field strength increases from 6.0 to 8.0 au. Instead, the transitions between the ground and higher excited states are strengthened. In addition, the plateau around the resonant peaks is broadened with higher laser intensity. The enlargement of the spectrum component near the emission energy of 254 au (energy difference between the ground and fourth excited state) is shown in figure 4(c) in units of the photon energy. The emission peaks are separated by $2\hbar\omega$ for $E = 6.0$ au. The existence of plateau here can be explained from the aspect of the Stark broadening of the excited states with narrow continuum energy band structures in the ultraintense laser field. This Stark broadening is more obvious for the highly excited states as indicated in figure 4(a). One can also see the Stark shift [25] and the energy level splitting in figure 4(c) when the electric field strength of the laser increases to $E = 8.0$ au. This splitting of the excited state is also a relativistic effect due to the additional spin-orbit coupling and becomes larger by increasing the laser intensity [13].

The parameter $eE/m\omega = 105.26 \approx 0.768c$ for the lower laser intensity here ($E = 6.0$ au) indicates that the

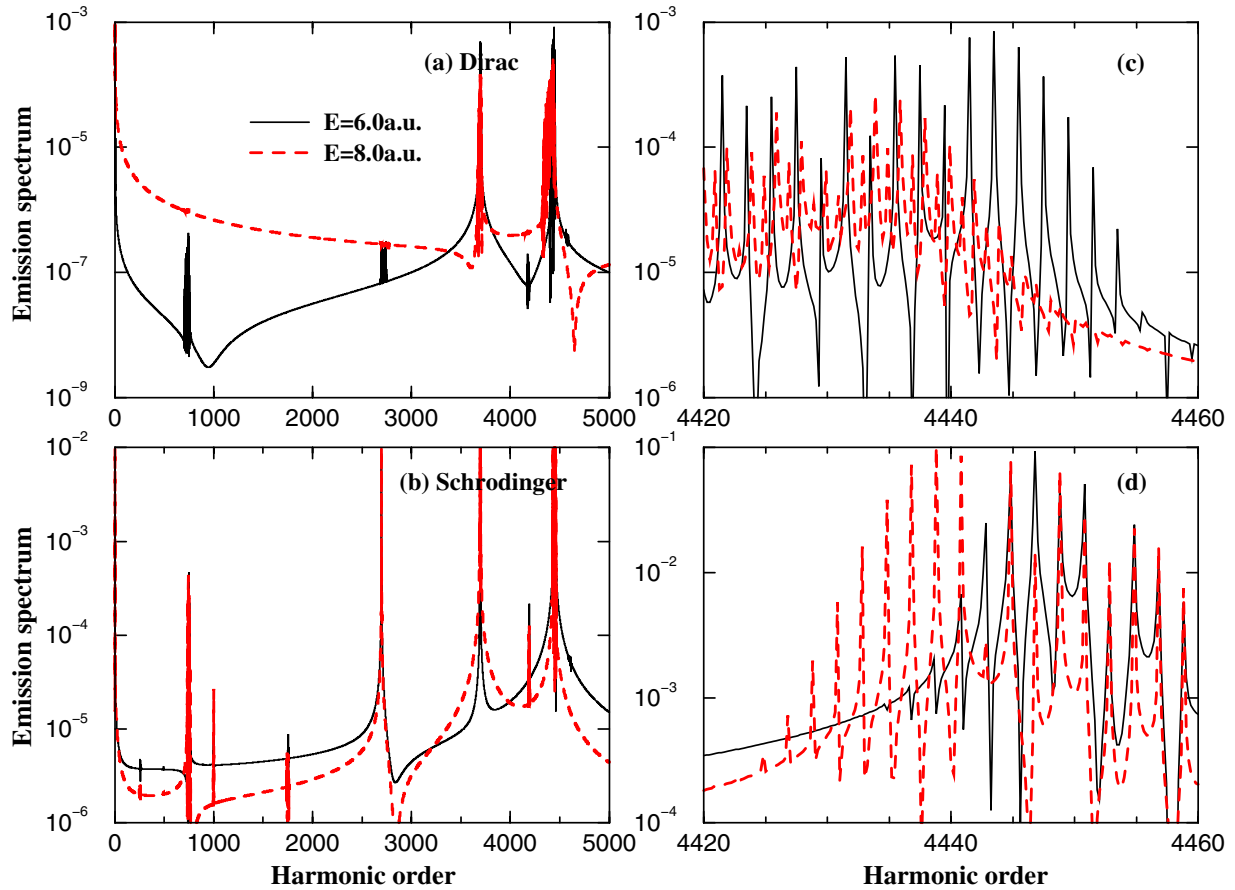


Figure 4. The emission spectrum for the ionic model $V(x) = -24/\sqrt{x^2 + 0.0035}$ calculated from 1D (a) TDDS and (b) TDSE in the 800 nm infrared laser field with $E = 6.0$ au (black solid line) and $E = 8.0$ au (red dashed line). Panels (c) and (d) are enlargements of panels (a) and (b) around the emission energy of 254 au.

non-relativistic treatment cannot produce reliable results. The corresponding emission spectrum with the same parameters by solving the 1D dipole approximation TDSE is shown in figure 4(b). Comparing with the relativistic results, the ionization probability is much smaller. We can also see that the Stark broadening is much weaker than that predicted in the relativistic calculation. The Stark shift of the excited state is also weakened and can be hardly seen for the fourth excited states as shown in figure 4(d). Furthermore, the splitting of the excited state disappears because the spin-orbit coupling cannot be considered in the TDSE.

According to the non-relativistic theory, the tunneling ionization will dominate when the Keldysh parameter, defined as $\gamma = \sqrt{I_p/2U_p}$, is much less than 1 [8]. This condition has been satisfied for the parameters chosen in figure 4, while it is obvious that the multi-photon ionization still dominates here. Only emissions below the ionization threshold can be observed and no tunneling happens here. This may be explained by the following: (i) the Keldysh parameter is deduced by comparing the tunneling time and the optical cycle of the laser field; the former parameter is defined without considering the height of the potential barrier and the mass changes of the electron regarding speed; and (ii) for a highly charged ion, because the potential barrier for the tunneling ionization is much higher than for the neutral systems, there may be situations where the tunneling ionization probability is very small while the tunneling time calculated typically is

much less than the oscillation time of the laser. For this kind of case, the multi-photon resonant excitations take place much faster than those of the tunneling ionization [24]. When the speed of the electron is close to that of light, the conditions for the tunneling ionization should be defined in relativistic theory with proper consideration of the height and shape of the potential barrier.

5. Conclusion

The electronic dynamics of the highly charged ions in an ultraintense laser field are investigated by solving the TDDE. One can see the competition between the strength of the ionic core field and the laser field from the trajectory of the electron. For highly charged ions, clear features of the tunneling ionization cannot be seen even when the Keldysh parameter is much less than 1. For the infrared laser field of $E = 8.0$ au, we have only seen the below-threshold emission caused by the resonant transitions between the bound states when the nuclear charge $Z = 24$. The relativistic effects on the excited states, including the Stark broadening and shift and the energy level splitting, can also be seen in the resonant multi-photon emission spectra. To obtain harmonics above the ionization threshold, one can adopt a laser field with higher frequency.

Acknowledgments

This work was supported by the National Natural Science Foundation of China under grant no. 10734140 and the National Basic Research Program of China (973 Program) under grant no. 2007CB815105.

References

- [1] Papadogiannis N A, Witzel B, Kalpouzos C and Charalambidis D 1999 *Phys. Rev. Lett.* **83** 4289
- [2] Burnett K, Reed V C and Knight P L 1993 *J. Phys. B: At. Mol. Phys.* **26** 561
- [3] Krause J L, Schafer K J and Kulander K C 1992 *Phys. Rev. Lett.* **68** 3535
- [4] Kruit P, Kimman J, Muller H G and Van der Wiel M J 1983 *Phys. Rev. A* **28** 248
- [5] Yang B, Schafer K J, Walker B, Kulander K C, Agostini P and DiMauro L F 1993 *Phys. Rev. Lett.* **71** 3770
- [6] Millack T and Maquet A 1993 *J. Mod. Opt.* **40** 2161
- [7] Zhou Z and Yuan J 2008 *Phys. Rev. A* **77** 063411
- [8] Keldysh L V 1965 *Sov. Phys.—JETP* **20** 1307
- [9] Rouyer C, Mazataud É, Allais I, Pierre A, Seznec S, Sauteret C, Mourou G and Migus A 1993 *Opt. Lett.* **18** 214
- [10] Yamakawa K, Shiraga H and Kato Y 1991 *Opt. Lett.* **16** 1593
- [11] Rathe U W, Keitel C H, Protopapas M and Knight P L 1997 *J. Phys. B: At. Mol. Phys.* **30** L531
- [12] Corkum P B 1993 *Phys. Rev. Lett.* **71** 1994
- [13] Hu S X and Keitel C H 2001 *Phys. Rev. A* **63** 053402
- [14] Mokler P H and Stöhlker T 1996 *Adv. At. Mol. Opt. Phys.* **37** 297
- [15] Kubodera S, Nagata Y, Akiyama Y, Midorikawa K, Obara M, Tashiro H and Toyoda K 1993 *Phys. Rev. A* **48** 4576
- [16] Braun J W, Su Q and Grobe R 1999 *Phys. Rev. A* **59** 604
- [17] Krekora P, Su Q and Grobe R 2004 *Phys. Rev. Lett.* **92** 040406
- [18] Gerritsma R, Kirchmair G, Zähringer F, Solano E, Blatt R and Roos C F 2010 *Nature* **463** 68
- [19] Javanainen J, Eberly J H and Su Q 1988 *Phys. Rev. A* **38** 3430
- [20] Liu W C and Clark C W 1992 *J. Phys. B: At. Mol. Phys.* **25** L517
- [21] Vázquez de Aldana J R and Roso L 2000 *Phys. Rev. A* **61** 043403
- [22] Grochmalicki J, Lewenstein M and Rzazewski K 1991 *Phys. Rev. Lett.* **66** 1038
- [23] Hu S X and Keitel C H 1999 *Europhys. Lett.* **47** 318
- [24] Hu S X, Starace A F, Becher W, Sandner W and Milošević D B 2002 *J. Phys. B: At. Mol. Phys.* **35** 627
- [25] Casu M and Keitel C H 2002 *Europhys. Lett.* **58** 496